Proceedings of the ASME 28th International Conference on Ocean, Offshore and Arctic Engineering
OMAE2009
May 31 - June 5, 2009, Honolulu, Hawaii, USA

OMAE2009-79392

A JOINT NUMERICAL AND EXPERIMENTAL STUDY OF A SURGING POINT ABSORBING WAVE ENERGY CONVERTER (WRASPA)

Majid A. Bhinder
Centre For Mathematical Modelling And Flow Analysis
Manchester Metropolitan University
Manchester, United Kingdom

Clive G. Mingham
Centre For Mathematical Modelling And Flow Analysis
Manchester Metropolitan University
Manchester, United Kingdom

Derek M. Causon
Centre For Mathematical Modelling And Flow Analysis
Manchester Metropolitan University
Manchester, United Kingdom

Mohammad T. Rahmati
Lancaster University, Faculty of Science and Technology
Lancaster, United Kingdom

George A. Aggidis
Lancaster University, Faculty of Science and Technology
Lancaster, United Kingdom

Robert V. Chaplin
Lancaster University, Faculty of Science and Technology
Lancaster, United Kingdom

ABSTRACT

This paper presents the findings from using several commercial computational fluid dynamics codes in a joint numerical and experimental project to simulate WRASPA, a new wave energy converter (WEC) device.

A series of fully 3D non-linear simulations of WRASPA are presented. Three commercial codes STAR-CCM, CFX and FLOW-3D are considered for simulating the WRASPA device and final results are presented based on the use of Flow-3D. Results are validated by comparison to experimental data obtained from small scale tank tests undertaken at Lancaster University (LU).

The primary aim of the project is to use numerical simulation to optimize the collector geometry for power production over a range of likely wave climates. A secondary aim is to evaluate the ability of commercial codes to simulate rigid body motion in linear and non-linear wave climates in order to choose the optimal code with respect to compute speed and ease of problem setup. Issues relating to the ability of a code in terms of numerical dissipation of waves, wave absorption, wave breaking, grid generation and moving bodies will all be discussed.
The findings of this paper serve as a basis for an informed choice of commercial package for such simulations. However the capability of these commercial codes is increasing with every new release.

INTRODUCTION

The development of economical technologies for generating power from renewable sources is a primary objective of modern society. Recent political support for exploring renewable energy sources has encouraged scientists to conduct further research towards their current findings. As a renewable energy source, wave energy has an intensive record of research and development which has spanned three decades. Other renewable sources include solar, hydroelectric, marine current and wind.

This paper has emerged from the numerical simulations of a new wave energy converter named WRASPA, a point absorber WEC intended to be deployed at a water depth of 20-50m. WRASPA is an acronym for **W**ave-driven **R**esonant, **A**rcuate-action, **S**urging **P**ower **A**bsorber.

WRASPA, invented at LU, will produce an estimated power output of 2MW in the North Atlantic. In response to incident waves a collector body moves around a pivot above the sea bed and energy is extracted from the resulting surging motion [1- 5]. Numerical models not only allow assessment of various scales at relatively low costs but also provide for an optimized

configuration in early stage models. Numerical/mathematical modelling allows several designs to be tested in the fastest way possible. In this paper, propagation of linear wave has been simulated in a numerical wave tank (NWT). The aim is to record the coupled motion of the wave energy converter WRASPA in response to the incoming waves in the NWT. A sketch of the device in incident waves is depicted in Figure 1.

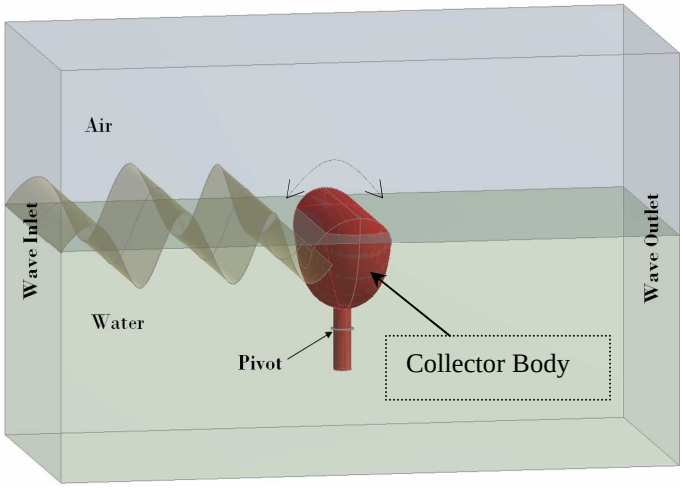

Figure1: A depiction of WRASPA's fixed axis pitch motion against incident waves.

EXPERIMENTAL SETUP:

Wave tank tests have been carried out at Lancaster University on a 1/100th scale model of the device to evaluate its performance. The model and the apparatus used are shown in Figure 2.

The collector body (Fig1-2) has a streamlined shape to give large amplitudes of motion to extract energy from waves [2]. The pivot point is adjustable and can be varied between 200-300mm below the water level. The position of centre of pressure can also be varied by changing the vertical position of the collector body on the arm. A reasonably linear relationship between the wave and pitch amplitudes is found for wave amplitudes up to 25 mm with corresponding pitch angles in excess of 0.45 rad. The wave force vector on the collector and the pitch of the device were measured for various body immersions and pivot depths. More detail of the wave tank experiment can be found at [1-3].

Instantaneous position (pitch motion) of $1/100^{th}$ scale model of WRASPA in small amplitude regular wave was recorded (Figure 10) in the absence of any control forces/torque.

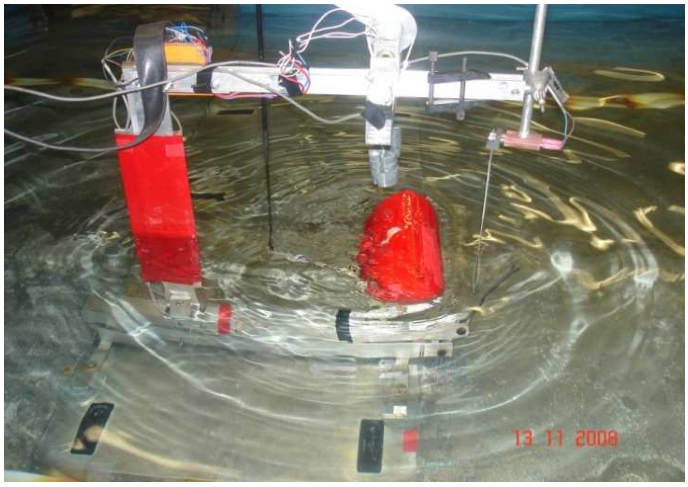

Figure 2: 1/100th scale model and the rig in experimental wave tank

NUMERICAL MODELLING:

Mathematically, fluid flow and rigid body motion is described by conservation equations for mass and momentum. The equations for mass and momentum result in a system of four coupled nonlinear partial differential equations known as the Navier-Stokes equations. This system can be solved analytically only for simple flow problems. However, for complex problems, algebraic approximations are needed to solve the equations numerically. The turbulence associated with flow field can modelled via number of approximations including direct numerical simulation (DNS), large eddy simulation (LES) and Reynolds-averaged Navier-Stokes equation models (RANS). However available computer resources limit the use of DNS for only simple problems.

To simulate WRASPA, three commercial CFD (Computational Fluid Dynamics) packages CFX, STAR-CCM+ and Flow-3D was considered. All these packages are well known in the CFD community but their application for simulating water waves, particularly, involving moving rigid bodies, still needs to be explored further. All these packages are based on the Reynolds Averaged Navier Stokes (RANS) Equations. For modelling free surface waves each solver uses a slightly modified Volume of Fluid (VOF) model [7-9].

At the time of a preliminary analysis of WRASPA, STAR-CCM+ (v3.02) was found unable to handle the surging motion of a moving object whereas a later version (v3.04 and v3.06) claims this ability. However, this new capability needs more validation for the current application. It was observed that the output of control force/torque may also be an issue. Therefore, it was decided to continue the preliminary analysis of WRASPA using CFX and Flow-3D.

Linear waves were modelled as part of the preliminary analysis using all three codes. CFX and Starccm+ are unstructured codes and require finer mesh at the free surface to resolve it sufficiently to simulate wave propagation down the tank [7, 8].

Regular waves were successfully generated in CFX by defining velocities at the inflow boundary using linear wave theory. The mesh used with CFX is shown in Figure 3. It can be seen that at the free surface boundary a relatively fine cell layer is specified. This configuration was obtained by slicing the whole wave tank at the free surface position and then using an inflation layer of smaller prism cells.

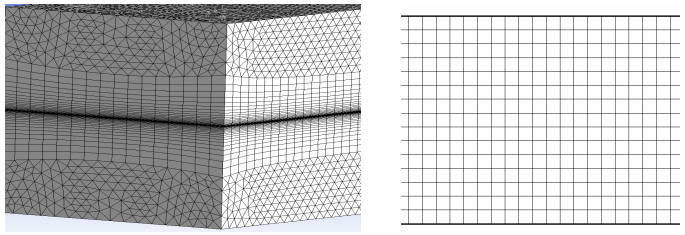

(a) (b)

Figure 3: Mesh structure used for linear wave simulations in 3D NWT using (a) CFX (b) Flow-3D

Figure 4 shows surface elevation of a single linear wave at two different instants obtained with CFX. It is noticed that decay of the wave amplitude along the tank is quite rapid due to numerical dissipation.

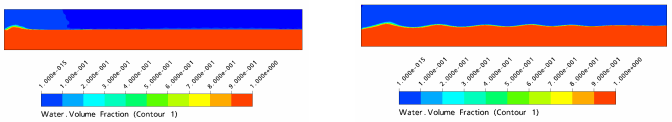

(a) (b)

Figure 4: Linear wave propagation in numerical wave tank of CFX at (a) 1.0s, (b) 9.25s

Flow-3D incorporates a different technique (TruVOF) to capture the free surface which does not need extra cells at the free surface (Figure 3b) and computes flow variables only within one fluid (water in our case) [9]. This major quality of Flow-3D reduces the computation time significantly.

A linear wave with the following definition parameters was simulated in Flow-3D and predicted surface elevations at two different locations from inlet boundary is presented in Figure 5.
Wave amplitude = 0.015m, Time period = 1s, Water Depth = 0.30m, Tank Dimensions = (12.5m, 0.45m, 2.5m).

Computational Specifications = Intel(R) Core(TM)2 Duo CPU E6750@2.66GHz , 8GB of RAM. Total Number of Cells = 605456, Smallest Cell Size = 2.9976E-02.
Time taken by solver to compute a 20 seconds case = 2.030E+04(seconds) = 2:08 hr

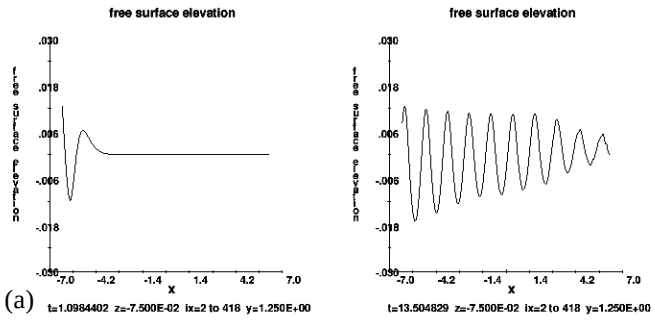

(a)

Figure 5: Flow-3D Results of Surface Elevation at (a) t=1.0s (b) t=13.50s

CFX uses a deforming mesh to handle a moving object which requires large amounts of computation time as well as extra effort in mesh generation as the user needs to fulfill imposed cell requirements for a moving/deforming mesh.

Flow-3D uses a General Moving Object (GMO) model to simulate three-dimensional coupled/prescribed motion of any arbitrary shaped body in a fixed computational mesh within a wave tank (computational domain).

It is observed that Flow-3D is relatively much in-expensive in terms of computational time for not only wave's propagation but also for modelling moving object such as WRASPA with a great deal of accuracy. Hence Flow-3D was found to be the best suited code for the present project and the final numerical simulations are being conducted only using Flow-3D.

Flow-3D uses a unique technique named FAVOR^{TM} to describe geometric objects in a computational domain [9] which is based on the concept of area fraction (AF) and volume fraction (VF) in a rectangular structured mesh. The VF is defined as the ratio of open volume to the total volume in a cell whereas three AF's (AFR, AFB, AFT) are defined for three cell faces respectively in the direction of increasing cell-index as the ratio of the open area to the total area. This FAVOR^{TM} technique works well with complex geometries by introducing the effects of AF and VF into the conservation equations of fluid flow. This technique has led to the successful development of a general moving object (GMO) capability which in principle permits the modelling of any type of rigid body motion (six degree of freedom, fixed axis and fixed point) on a fixed-mesh.

This particular simulation is the application of this GMO model to a fixed axis dynamically coupled motion of WRASPA. Solver calculates AF and VF at each time step which describes object's motion through a fixed-rectangular mesh. Hydraulic, gravitational, and control forces and torques are calculated and equations of motion for the rigid body are solved explicitly for translational and rotational velocities of moving objects under a

coupled motion. Further detail of mathematical model used within Flow-3D is given in the next sub-section.

EQUATIONS OF MOTION FOR A MOVING RIGID BODY IN FLOW-3D:

Any rigid body motion can be considered partially as translational and partially as rotational motion. The velocity of any point on a moving body is equal the velocity of the arbitrary base point plus the velocity due to the rotation of the object about that arbitrary point. For 6-DOF motion, the GMO model considers moving body's mass centre G as the base point. The equations of motion governing two separate motions for 6-DOF motion are [12].

$$\vec{F} = m\frac{d\vec{V_G}}{dt} \tag{1}$$

$$\vec{T_G} = [J].\frac{d\vec{\omega}}{dt} + \vec{\omega}\times\left([J].\vec{\omega}\right) \tag{2}$$

Where F is the total force, m is rigid body's mass, T_G is the total torque about G and $[J]$ is moment of inertia tensor about G in a body fitted reference system. The total force and total torque are calculated as the sum of several components as

$$\vec{F} = \vec{F_g} + \vec{F_h} + \vec{F_c} + \vec{F_{ni}} \tag{3}$$

$$\vec{T_G} = \vec{T_g} + \vec{T_h} + \vec{T_c} + \vec{T_{ni}} \tag{4}$$

where $\vec{F_g}$ is gravitational force, $\vec{F_h}$ is hydraulic force due to the pressure field and wall shear forces on the moving object, $\vec{F_c}$ is the net control force prescribed to control or restrict the rigid body's motion and $\vec{F_{ni}}$ is the non-inertial force if a rigid body moves in a non-inertial space system. In our case, $\vec{F_{ni}}$ is not present. Similarly, $\vec{T_G}$, $\vec{T_g}, \vec{T_h}, \vec{T_c}$ and $\vec{T_{ni}}$ are the total torque, gravitational torque, hydraulic torque, control torque and non-inertial torque about the mass centre respectively.

The continuity and momentum equations for a moving object and the relative transport equation for the volume of fluid (VOF) function are

$$\frac{V_f}{\rho}\frac{\partial \rho}{\partial t} + \frac{1}{\rho}\nabla.(\rho\vec{u}A_f) = -\frac{\partial V_f}{\partial t} \tag{5}$$

$$\frac{\partial \vec{u}}{\partial t} + \frac{1}{V_f}(\vec{u}A_f.\nabla\vec{u}) = -\frac{1}{\rho}\left[\nabla p + \nabla.\left(\tau A_f\right)\right] + \vec{G} \tag{6}$$

$$\frac{\partial F}{\partial t} + \frac{1}{V_f}\nabla.(F\vec{u}A_f) = -\frac{F}{V_f}\frac{\partial V_f}{\partial t} \tag{7}$$

where ρ is the density of the fluid (water in our case), $\vec{u}$ fluid velocity, V_f volume fraction, A_f area fraction, p pressure, τ viscous stress tensor, G gravity and F is fluid fraction.
In the case of coupled GMO's motion, equations (1) and (2) are solved at each time step and the location of all moving objects is recorded and the area and volume fractions updated using the FAVOR technique. Equations (5) and (7) are solved with the source term $\left(-\frac{\partial V_f}{\partial t}\right)$ on the right-hand side which is computed as

$$-\frac{\partial V_f}{\partial t} = \overrightarrow{U_{obj}} \cdot \vec{n} S_{obj} \Big/ V_{cell} \tag{8}$$

where S_{obj} is the surface area, $\vec{n}$ surface normal vector, $\overrightarrow{U_{obj}}$ is the velocity of the moving object at a mesh cell and V_{cell} is the total volume of the cell as drawn in Figure 6.

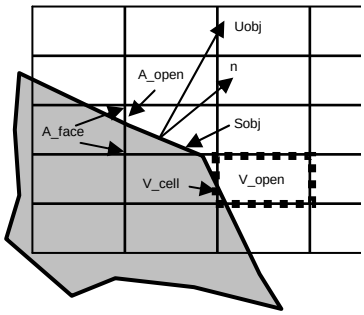

Volume fraction:
Vf=V_open/V_cell
Area fraction:
Af= A_open/A_face
Source Term:
Uobj.nSobj/V_cell

Figure 6: Schematic explaining the source term.

The explicit GMO method solves equations (1) and (2) according to the following discretized equations

$$\vec{F_h}^n + \sum\vec{F}_i = m\left(\frac{\vec{V}_G{}^{n+1} - \vec{V}_G{}^n}{\Delta t}\right) \tag{9}$$

$$\vec{T_h}^n + \sum\vec{T}_i = [J]\cdot\left(\frac{\vec{\omega}^{n+1} - \vec{\omega}^n}{\Delta t}\right) + \vec{\omega}^n \times\left([J]\cdot\vec{\omega}^n\right) \tag{10}$$

The implicit GMO method used for simulating the moving device solves equations (1) and (2) implicitly using the following numerical scheme.

$$\vec{F}_h^{\,n+1} + \sum \vec{F}_i = m\left(\frac{\vec{V}_G{}^{n+1} - \vec{V}_G{}^{n}}{\Delta t}\right) \quad (11)$$

$$\vec{T}_h^{\,n+1} + \sum \vec{T}_i = [J]\cdot\left(\frac{\vec{\omega}^{\,n+1} - \vec{\omega}^{\,n}}{\Delta t}\right) + \vec{\omega}^{\,n} \times \left([J]\cdot\vec{\omega}^{\,n}\right) \quad (12)$$

where the upper index denotes the time step, $\sum \vec{F}_i$ and $\sum \vec{T}_i$ is the sum of all the force and torque components respectively excluding the hydraulic components. At each time step after $\vec{V}_G{}^{n+1}$ and $\vec{\omega}^{\,n+1}$ are computed in this manner, the fluid velocity and pressure field are calculated by iteratively solving the continuity and momentum equations.

At each time step the main computational procedure is:

1. using pressure and velocity from the previous step calculate the force and torque for coupled motion of the moving objects.
2. calculate the mass centre velocity and angular velocity under coupled motion explicitly using equations (9) and (10).
3. record the location of moving object.
4. update the volume and area fractions.
5. calculate the source term $\left(-\frac{\partial V_f}{\partial t}\right)$ using equation (8).
6. perform one predictor-correction iteration for the fluid velocity and pressure using the descretized form of equations (5) and (6). If convergence is achieved go to step 10.
7. update the force and torque for all moving objects under coupled motion using the newly updated pressure and fluid velocity found in step 6. Apply under-relaxation to the fluid velocity and pressure if necessary.
8. update the mass centre velocity and angular velocity for theh moving objects under coupled motion using the implicit scheme in equations (11) and (12) with newly updated force and torque. Apply under-relaxation if necessary.
9. back to Step 5.
10. Proceed to the next step.

Further detail about underlying mathematical model and numerical scheme is available in [9].

SIMULATION SETUP OF WRASPA IN FLOW-3D AND RESULTS:

Flow-3D uses a structured mesh which, relatively, requires very little time and is fairly easy to generate. It allows nested mesh blocks to add more cells in areas of interest to provide an accurate flow description. The mesh structure generated within Flow-3D's preprocessor is shown in Figure 7.

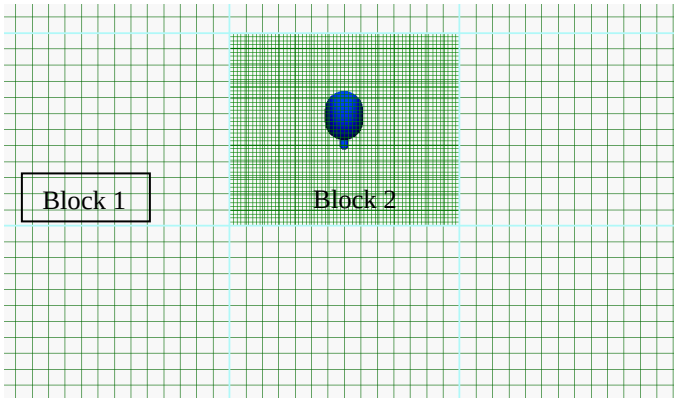

Figure 7: (Side View) Nested mesh blocks used for computing flow field in Flow-3D.

A linear wave boundary condition is set by prescribing velocity components using linear wave theory. Flow-3D's wave maker boundary has already been used and tested by [11]. The turbulence model used for the final simulations is the RNG (Renormalization group) model preferred by [9].

Flow-3D offers a choice of explicit and implicit GMO model. The lower density of the WRASPA device (compared to the surrounding fluid's density) has led to the choice of an implicit GMO model [9]. It was observed that the implicit method showed high stability and good efficiency for our problem. In the implicit method the force and torque from the current time step rather than previous time step are used to solve the equations of motion for the rigid body. At each time step, the hydraulic forces and torques, mass centre velocities and angular velocities of the moving object, velocity and pressure distributions in the fluid are calculated iteratively in a coupled manner.

The case shown in Figure 8-9 was simulated with wave amplitude of 0.01m, time period 1s and water depth 0.42m. The computational domain was composed of 971924 cells, with the smallest cell being 0.01 m. A smaller cell size was used within mesh block2 which surrounds the device with the largest cell size in the outer block1 as illustrated in Figure 7.

The computational domain, having dimensions of 12 m x 2.5m x 0.738 m (length x width x height), was discretized into 971924 total cells. An outflow boundary condition, coupled with bigger stretched adjacent cells, was used at the

downstream end to minimize reflected waves [9]. For a 30 seconds run, Flow-3D's cpu time was found to be 2 Days (approx).

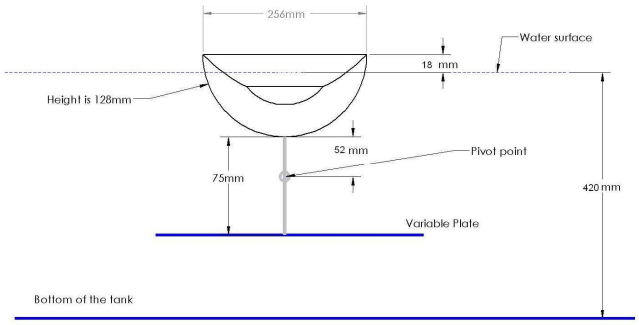

Figure 8: Schematic showing a front view of WRASPA in the Numerical Wave Tank.

Variables of interests include the rotational angle of the device, hydraulic torque and the amplitude of the incident wave. Velocity profiles from this simulation at two different instants are shown in Figure 9 and corresponding rotational angle of device is plotted against experimental values (Figure 10).

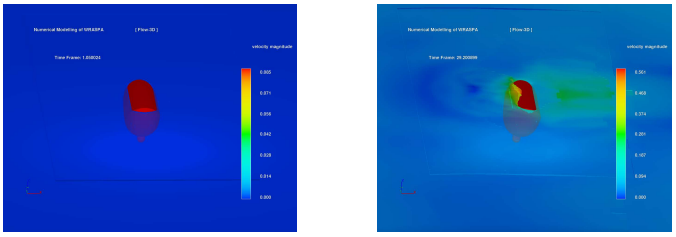

(a) (b)

Figure 9: Velocity profiles of incident waves and response of WRASPA using Flow-3D at time (a) 1.05s (b) 29.2s

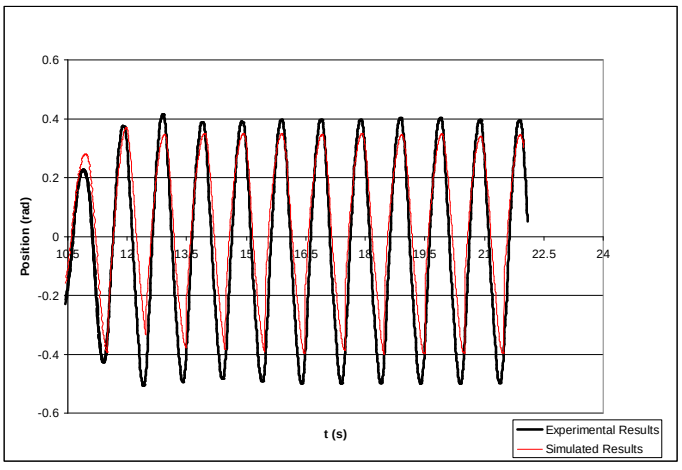

Figure 10: Comparison of Experimental and Numerical time history of Rotational Angle (in radian) of device.

CONCLUSIONS AND FURTHER WORK

It is found that numerical results are in reasonable agreement with experimental values. Owing to mesh size and theoretical assumptions made for mathematical modelling, there is a little difference between measured and simulated values.

The angular velocity of device computed from available instantaneous values of its rotational angle can be used with hydraulic torque to obtain corresponding power [2, 3].

Although linear waves can be simulated in CFX , dissipation rate was found to be quite rapid and high. Flow-3D's one fluid method keeps free surface interface sharp without requiring extra cells at free surface and it is observed that with Flow-3D the computation time is significantly reduced compared to the other codes. Flow-3D uses a built-in Outflow boundary condition which can be used to avoid wave reflections. However to capture the rigid body's geometric shape accurately, a much finer mesh around rigid objects is needed in computational domain of Flow-3D. The current difference between simulated and measured data might also be the cause of this rendered geometry of the collector body and will be investigated further as part of future work.

It is found that the difference between simulated and experimental values of pitch motion of device is small for small amplitude waves (such as 10mm). However this difference increases with the increase of wave amplitude. Thus a part of further work will be devoted to this investigation. Further work would also involve investigating experimental results of non-linear waves and modelling controlled motion of WRASPA in linear and non-linear wave climate. This control system applies constant opposing torque to restrict WRASPA's surging motion.

ACKNOWLEDGMENTS

The authors would like to acknowledge funding for this project from Joule Centre (www.joulecentre.org) grant no. JIRP306/02. The authors appreciate technical support from Flow Science Inc. during the training session in Santa Fe New Mexico, USA.

REFERENCES

[1] R. V. Chaplin and M. S. Folley. "Sea-bed devices-technical comparisons of existing and new types," 4th European Wave Energy Conference, Patras, 1998.

[2] Chaplin, R.V. and G.A. Aggidis, "WRASPA: Wave Interactions and Control in a new Pitching-Surge Point-Absorber Wave Energy Converter," 7th European wave and tidal energy conference, Portugal, 2007.

[3] Chaplin R.V. and Aggidis G.A., “An Investigation into Power from Pitch-Surge Point-Absorber Wave Energy Converters,” published by IEEE, Clean Electrical Power, ICCEP '07, 2007.

[4] M.T. Rahmati, G. A. Aggidis and R.V. Chaplin, “Investigating Pitching-Surge Power-Absorber Wave Energy Converters,” ASME POWER, Florida, USA, July 2008.

[5] M.T. Rahmati, G. A. Aggidis, R.V. Chaplin, “Tests on a Novel Pitching-Surge Wave Energy Converter,” World Renewable Energy Congress, Scotland, July 2008.

[6] Chaplin R.V. and Aggidis G.A., Rahmati, M.T., “WRASPA: (Wave-driven, Resonant, Arcuate action, Surging Power-Absorber),” Wave and Tidal Symposium, Renewable Energy Association, Cardiff, Wales, 2008.

[7] CD-Adapco, Star-CCM+ (v 3.02-3.06) Manual, 2008.

[8] ANSYS CFX (version 11) Documentation, 2008.

[9] Flow Science Inc. Flow-3D user manual, version 9.3.1, 2008.

[10] Hirt, C. W. and Nichols, B.D.: Volume of Fluid(VOF) method for the dynamics of free boundaries, J. Comp. Phys., 39,201-225, 1981.

[11] Choi, B.-H., Kim, D. C., Pelinovsky, E., and Woo, S. B.: Three-dimensional simulation of tsunami run-up around conical island, Coast. Eng., 54, 618-629, 2007.

[12] Goldstein H., Charles P. and Safko J., 2002, Classical Mechanics, Addison Wesley, Washington.